JOURNAL OF GUIDANCE, CONTROL, AND DYNAMICS
Vol. 18, No. 1, January–February 1995

High-Performance, Robust, Bank-to-Turn Missile Autopilot Design

Ching-Fang Lin*
American GNC Corporation, Chatsworth, California 91311
and
James R. Cloutier† and Johnny H. Evers‡
Wright Laboratories, Eglin Air Force Base, Florida 32542

Subjects related to a robust multivariable autopilot design are examined in this paper. First, a canonical robust control design formulation is introduced and is illustrated by formulating an integrated autopilot design problem. This formulation addresses the considerations of missile command following, model parameter variations, actuator dynamics, flexible dynamics, and parasitic feedback effects. Then, three robust autopilot designs for the HAVE DASH II missile system are executed. The controllers are solved using the generalized Hamiltonian approach which unifies a class of robust control designs in the same framework in terms of the formulation, data structure, and solution algorithm. The simulation shows that the designs achieve good response against significant kinematic and inertia couplings and aerodynamic parameter variations.

Nomenclature

A, B	= system state and input matrices
B_0, B_1	= control and exogenous input distribution matrices
C_0, C_1	= measurement and performance distribution matrices
D_{00}	= direct transmission matrix from u to y
D_{01}	= direct transmission matrix from w to y
D_{10}	= direct transmission matrix from u to z
D_{11}	= direct transmission matrix from w to z
g	= gravity constant
K	= controller
$l_\beta, l_{\delta r}, l_{\delta a}$	= rolling moment derivatives
$m_\alpha, m_{\delta e}, m_{\delta r}, m_{\delta a}$	= pitching moment derivatives
$n_\beta, n_{\delta r}, n_{\delta a}$	= yawing moment derivatives
$P(s)$	= augmented plant
$P_{yu}, P_{yw}, P_{zu}, P_{zw}$	= partitioning blocks of the augmented plant
p, q, r	= roll, pitch, and yaw rates
T_{zw}	= closed-loop transfer function from w to z
u	= control input
V_m	= total missile speed
w	= exogenous input
x	= state
y	= measurement (feedback) signal
$y_\beta, y_{\delta r}, y_{\delta a}$	= side force derivatives
z	= performance to be monitored (regulated)
$z_\alpha, z_{\delta e}, z_{\delta r}, z_{\delta a}$	= z-axis force derivatives
α, β, ϕ	= angle of attack, sideslip angle, and bank (roll) angle
α_i	= integral of α
Δ, Δ_i	= uncertainties
$\delta_a, \delta_e, \delta_r$	= roll, pitch, and yaw control deflections
ρ_i	= design parameters (weightings)
Θ	= missile pitch attitude angle

I. Introduction

TO take advantage of high-lift, low-drag, air intake, internal carriage, and low-observability features, missile airframes have undergone significant changes. As a result, new requirements and concerns are being imposed on the autopilot design. The asymmetric high-lift configuration gives the missile large maneuverability in its pitch plane, and the available load factor in the yaw plane is limited. Therefore, to track a target, a bank-to-turn (BTT) steering policy must be employed. The BTT control is realized via roll and pitch maneuvers. To achieve the desired orientation, a BTT missile rolls the normal plane to the desired direction. The magnitude of the maneuver is controlled by pitch control devices.

Unlike a skid-to-turn autopilot which can be designed with independent pitch, yaw, and roll channels, a BTT autopilot has to roll the normal lift plane to achieve a maneuver. This rolling motion induces Coriolis and gyroscopic couplings. Thus, the design problem is essentially multivariable in nature. This multivariable autopilot requires rapid and precise pitch and roll responses to intercept an incoming target. It is also imperative to maintain a small sideslip angle to fully utilize the air-breathing propulsion technique, to increase range, and to prevent departure.

In addition to stabilizing the multivariable coupled dynamics and to achieving a rapid response, the autopilot must also be robust against parasitic effects, such as radome swing, adaptive with respect to parameter variations, and compatible with other subsystems.

The availability of onboard hardware (computer) and software (advanced guidance law) and the demand to intercept a highly maneuverable target have increased the high-bandwidth requirement of the guidance loop. As a result, the autopilot is required to exhibit an even higher command response, bringing the missile's flexible effects into the design problem. This design concern is further jeopardized by the increment of fineness ratio. These flexible modes, if not stabilized, may degrade the tracking response or even cause instability. Moreover, these flexible dynamics are poorly known and are functions of time, flight condition, and maneuver level. The autopilot is then required not only to execute a rapid homing but also to stabilize elastic dynamics. In addition to elastic modes, the radome swing, especially at high altitude, also constitutes a parasitic feedback path and must be accounted for.

Requirements on the expanded flight envelope include longer range, faster speed, and higher altitude. These introduce large variations on the missile airframe parameters. The tracking performance of the missile, however, must be maintained throughout the flight envelope. That is, the autopilot must be able to adapt to the changes in the operating environment.

Finally, the autopilot must be compatible with other subsystems. Although it is desirable to have the autopilot respond as fast as

Received Aug. 23, 1993; revision received Aug. 17, 1994; accepted for publication Aug. 19, 1994.

*President. Associate Fellow AIAA.
†Senior Scientist, Armament Directorate. Associate Fellow AIAA.
‡Program Manager, Autopilot Program, Armament Directorate.

possible, if the autopilot bandwidth is too high it may amplify the seeker noise and degrade the tracking performance. Similarly, a large guidance gain may result in rapid homing. Yet, if the guidance gain is too large, it may saturate the autopilot and cause instability. It is thus required to tradeoff tracking response, noise effects, and stability from an overall system design perspective.

All of these requirements have stressed the use of classical one-loop-at-a-time design methods to their limit. On the other hand, multivariable robust control design methods offer several advantages, which include[1-7]: minimizing the use of gain scheduling mechanisms, taking advantage of coupling effects, offering design insights such as fundamental limitations and performance/robustness tradeoffs, and accounting systematically for modeling uncertainties. Despite the promised advantages, applications of multivariable robust control methods to missile systems remain limited. This is largely due to the fact that multivariable robust design methods fail to address practical missile-oriented issues.

The objective of this paper is to formulate and design a missile autopilot using current multivariable control methodology. The paper is organized into two parts: design formulation and design results demonstration. In Sec. II, a general robust control design formulation is presented and the procedure to establish a robust autopilot design formulation in this canonical form is illustrated. In Sec. III, the missile dynamic models are introduced first. Then a class of robust designs have been applied to the HAVE DASH II missile autopilot design. Among the designs are the linear quadratic Gaussian autopilot, generalized singular linear quadratic (GSLQ) autopilot, and H^∞ autopilot. All of the designs are formulated in the canonical form and solved based on the generalized Hamiltonian formulation. The robust performance of each design is visible from the simulation results. The blending of different design approaches provides the potential of reducing conservatism in using a particular design method.

II. Canonical Design Formulation

A general canonical form for the feedback system design problem is discussed in this section. It is shown that the design concerns of the missile autopilot can be systematically formulated using this canonical framework. As a result, autopilot design tradeoffs can be carried out in a highly organized manner. The canonical setting of the control design block diagram is shown in Fig. 1, where the augmented plant dynamics is given by

$$\begin{bmatrix} z \\ y \end{bmatrix} = \left[\begin{array}{c|c} P_{zw} & P_{zu} \\ \hline P_{yw} & P_{yu} \end{array}\right] \begin{bmatrix} w \\ u \end{bmatrix} = P(s) \begin{bmatrix} w \\ u \end{bmatrix} \tag{1}$$

The transfer functions $P_{zw}(s)$, $P_{zu}(s)$, $P_{yw}(s)$, and $P_{yu}(s)$ are derived from the plant dynamics, sensor/actuator dynamics, exogenous signal models, weightings, and interconnection topology. The design objective is to synthesize a controller $K(s)$ such that the design requirements are satisfied. Typical design requirements include internal stability, robustness, and performance, among many others. The overall input-output map, i.e., the transfer function from w to z, is a linear fractional map,

$$F_l(P, K) = P_{zw} + P_{zu}(I - KP_{yu})^{-1}KP_{yw} \tag{2}$$

provided that $[I - K(\infty)P_{yu}(\infty)]^{-1}$ exists. The linear fractional map (2) contains performance measures such as stability, robustness, command tracking response, actuator activity, and so forth, as its entries. The objectives in the autopilot loop design are to achieve 1) a satisfactory acceleration command response, 2) robustness against unmodeled flexible dynamics, 3) robustness against actuator uncertainty, and 4) insensitivity against aerodynamic parameter variations. The list is not exhaustive. Requirements such as time delay and nonlinearities may need to be considered. These nonlinearities include fin position and actuator rate limits, gear backlash, and gyroscopic couplings induced by the missile's roll rate. The design objectives can be characterized using the canonical form as follows. Consider the augmented system block diagram in Fig. 2, in which G is the nominal plant model given by $G = D + C(Is - A)^{-1}B$, K_2 is the feedback controller, and K_1 is the feedforward controller.

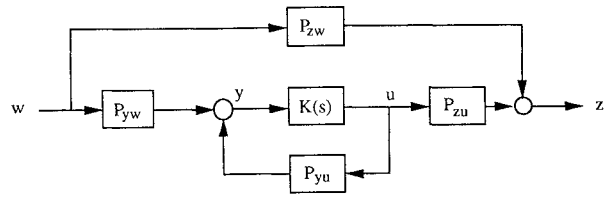

Fig. 1 Canonical setting of control design diagram.

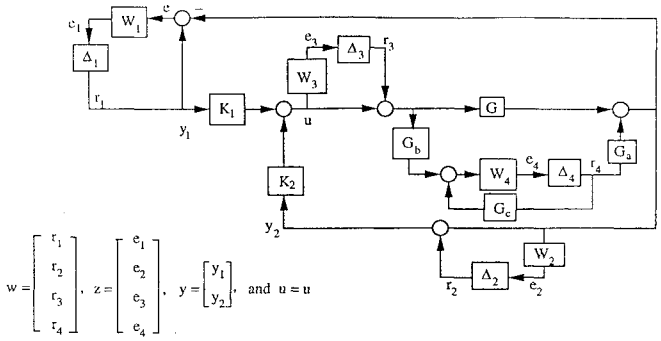

Fig. 2 Design formulation of the autopilot loop.

To achieve a satisfactory command following so that the missile can successfully track and intercept the target, the transmission from the guidance command r_1 to the tracking error e must be minimized. To better represent physical significance and to reduce conservatism in a practical design, a frequency-dependent weighting is generally introduced to filter r_1 and e. The frequency-dependent weighting W_1 is selected to reflect the frequency contents of the command response. Since the command response is of limited bandwidth, W_1 must also be a low-pass filter. Letting $e_1 = W_1 e$, the transfer function from r_1 to e_1 can be written as

$$\begin{aligned} e_1 &= \left[W_1 - W_1 G(I - K_2 G)^{-1} K_1\right] r_1 \\ &= \left\{ W_1 - W_1 G\left(I - [K_1 \quad K_2] \begin{bmatrix} 0 \\ G \end{bmatrix} \right)^{-1} [K_1 \quad K_2] \begin{bmatrix} I \\ 0 \end{bmatrix} \right\} r_1 \end{aligned} \tag{3}$$

Clearly, this is a linear fractional map with

$$P_{zw} = W_1, \qquad P_{zu} = -W_1 G, \qquad P_{yw} = \begin{bmatrix} I \\ 0 \end{bmatrix} \tag{4}$$

$$P_{yu} = \begin{bmatrix} 0 \\ G \end{bmatrix}, \qquad K = [K_1 \quad K_2] \tag{5}$$

Minimizing the transfer function from r_1 to e_1 results in a good command response. Another design uncertainty is represented by the missile flexible dynamics. The design concern due to unmodeled dynamics and sensor noise is taken into account by penalizing the transmission from r_2 to e_2. The weighting W_2 is selected to characterize the unmodeled flexible dynamics. Since the flexible dynamics are less known (more uncertain) at higher frequencies, W_2 is of a high-pass form. The transfer function from r_2 to e_2 is

$$\begin{aligned} e_2 &= W_2 G(I - K_2 G)^{-1} K_2 r_2 \\ &= W_2 G\left(I - [K_1 \quad K_2] \begin{bmatrix} 0 \\ G \end{bmatrix} \right)^{-1} [K_1 \quad K_2] \begin{bmatrix} 0 \\ I \end{bmatrix} r_2 \end{aligned} \tag{6}$$

Clearly, this is also in the form of Eq. (2) with

$$P_{zw} = 0, \qquad P_{zu} = W_2 G, \qquad P_{yu} = \begin{bmatrix} 0 \\ G \end{bmatrix}, \qquad P_{yw} = \begin{bmatrix} 0 \\ I \end{bmatrix} \tag{7}$$

This function is sometimes referred to as the weighted output complementary sensitivity function or robustness function. Minimizing this function is equivalent to increasing the robustness to the missile flexible dynamics.

The deflection and rate limits of the actuator must be considered in the autopilot design. An excessive autopilot gain may saturate the control surfaces and lead to undesirable consequences. Since the limits are not explicitly expressed in the linear model, a measure must be taken to reflect the actuator dynamics. The objective function is selected by penalizing the transmission from r_3 to e_3 to ensure the robustness at the actuator break point and to monitor the control activity. W_3 is also of a high-pass form so that it may reflect the high-frequency actuator uncertainty. This transfer function, referred to as the weighted input complementary sensitivity function, can be written as

$$e_3 = W_3\left(I - [K_1 \quad K_2]\begin{bmatrix}0\\G\end{bmatrix}\right)^{-1}[K_1 \quad K_2]\begin{bmatrix}0\\G\end{bmatrix}r_3 \tag{8}$$

Again, P_{zw}, P_{zu}, P_{yu}, and P_{yw} can be determined as

$$P_{zw} = 0, \qquad P_{zu} = W_3,$$
$$P_{yu} = \begin{bmatrix}0\\G\end{bmatrix}, \qquad P_{yw} = \begin{bmatrix}0\\G\end{bmatrix} \tag{9}$$

One last design concern in the autopilot loop is related to the parameter variations. Suppose that the system matrix is perturbed from A to $A+E_1\Delta_4W_4E_2$ for some (known) matrices E_1 and E_2 and unknown Δ_4. The perturbed transfer function, denoted as $G' = G + \Delta G$, can be written as

$$\begin{aligned} G &= D + C(Is - A - E_1\Delta_4W_4E_2)^{-1}B \\ &= \underbrace{D + C(sI - A)^{-1}B}_{G} + \underbrace{C(sI - A)^{-1}E_1}_{G_a}\Delta_4W_4 \\ &\times \left[I - \underbrace{E_2(sI - A)^{-1}E_1}_{G_c}\Delta_4W_4\right]^{-1}\underbrace{E_2(sI - A)^{-1}B}_{G_b} \end{aligned} \tag{10}$$

The effect of this parameter uncertainty can be characterized by the transfer function from r_4 to e_4. In the form of a linear fractional map, it is written as

$$e_4 = W_4\left\{G_c + G_b\left(I - [K_1 \quad K_2]\begin{bmatrix}0\\G\end{bmatrix}\right)^{-1}[K_1 \quad K_2]\begin{bmatrix}0\\G_a\end{bmatrix}\right\}r_4 \tag{11}$$

Therefore,

$$P_{zw} = W_4G_c, \qquad P_{zu} = W_4G_b, \qquad P_{yu} = \begin{bmatrix}0\\G\end{bmatrix},$$
$$P_{yw} = \begin{bmatrix}0\\G_a\end{bmatrix} \tag{12}$$

The stability margin of the closed-loop system is inversely proportional to the norm of this transfer function. In other words, by minimizing the norm of the transfer function of Eq. (11) subject to the stability requirement, the system can be made less sensitive to parameter variations.

By combining the preceding objective functions and placing them in the canonical setting, the plant with modeled uncertainty can be represented by

$$P = \left[\begin{array}{cccc|c} W_1 & 0 & -W_1G & -W_1G_a & -W_1G \\ 0 & 0 & W_2G & W_2G_a & W_2G \\ 0 & 0 & 0 & 0 & W_3 \\ 0 & 0 & W_4G_b & W_4G_c & W_4G_b \\ \hline I & 0 & 0 & 0 & 0 \\ 0 & I & G & G_a & G \end{array}\right] \tag{13}$$

and the controller to be synthesized is $K = [K_1 \quad K_2]$. The objectives are to make the (i, i) entries ($i = 1, 2, 3$, and 4) of $F_\ell(P, K)$ small. To see the generality of this canonical formulation, derivation of an integrated autopilot design formulation is illustrated subsequently.

A guidance loop is added to Fig. 2. The resulting augmented system block diagram is depicted in Fig. 3. The control design task will be extended to the guidance loop. A proportional navigation guidance (PNG) law will be used with the transfer function

$$G_F(s) = \frac{\Lambda V_c}{1 + \tau_a s}$$

where Λ is the navigation gain, τ_a the guidance constant, and V_c the closing speed. The closing speed, however, constitutes an uncertainty in the design because in most tactical missiles only the line-of-sight direction is measured. The closing speed is generally estimated by sophisticated filtering algorithms, thus inheriting a significant time delay. It is also a function of the target's maneuver. Therefore, the uncertainty due to closing speed is modeled as a multiplicative uncertainty and accounted for accordingly in the integrated autopilot design. The PNG law accepts the line-of-sight rate input from the seeker which is modeled as

$$G_s(s) = [s/(1 + \tau_s s)]$$

where τ_s is the seeker time constant. An additional parasitic feedback loop is considered in this integrated design. This parasitic feedback $G_i(s)$ includes the radome slope bias r_b, radome swing r_T, and leakage in the seeker isolation loop T_2:

$$G_i(s) = T_2s^2 + r_b \pm r_T/2$$

Note that the sign of the radome slope swing is indeterminate. In other words, the autopilot must be designed to be able to accommodate this sign variation. Also, this parasitic dynamic is driven by either the pitch or yaw rate. When the angular rates are contaminated by missile flexible effects, the tracking performance and stability margin are severely affected. The integrated robust autopilot design problem corresponding to Fig. 3 is formulated as a canonical design problem in which the augmented plant can be written as

$$P = \left[\begin{array}{cccccc|c} W_1 & -W_1G_FG_sG_i & -W_1G_vG & -W_1G_vG_a & -W_1G_FG_s & W_1G_F & -W_1G_vG \\ 0 & 0 & W_2G & W_2G_a & 0 & 0 & W_2G \\ 0 & 0 & 0 & 0 & 0 & 0 & W_3 \\ 0 & 0 & W_4G_b & W_4G_c & 0 & 0 & W_4G_b \\ 0 & I & G & G_a & 0 & 0 & G \\ 0 & -G_sG_i & -G_sG_iG & -G_sG_iG_a & -G_s & 0 & -G_sG_iG \\ \hline I & -G_FG_sG_i & -G_FG_sG_iG & -G_FG_sG_iG_a & -G_FG_s & G_F & -G_FG_sG_iG \\ 0 & I & G & G_a & 0 & 0 & G \end{array}\right] \tag{14}$$

where $G_v = I + G_FG_sG_i$. The additional uncertainty blocks, Δ_5 and Δ_6, in the attitude loop are used to account for radome slope error and closing speed uncertainty, respectively. In the computation of the controller, the improper character of $G_i(s)$ is taken into

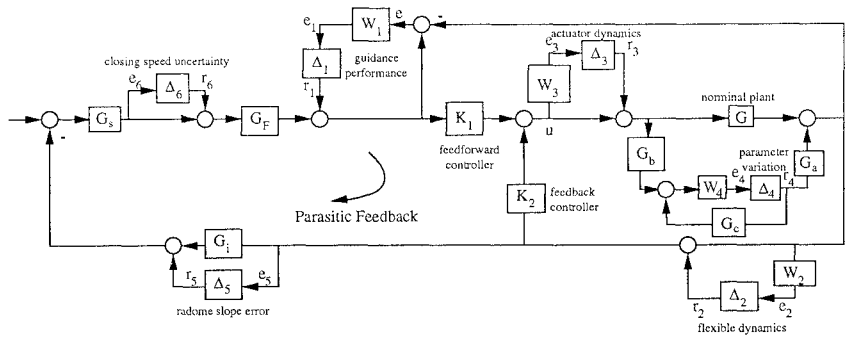

Fig. 3 Integrated autopilot design formulation.

consideration by either selecting appropriate weightings or utilizing numerical techniques.

A. Synergistic Robust Control Design

We will limit our attention to a linear, time-invariant, proper plant $P(s)$. It is assumed that $P(s)$ admits the following state space realization:

$$P(s) = \left[\begin{array}{c|c} P_{zw}(s) & P_{zu}(s) \\ \hline P_{yw}(s) & P_{yu}(s) \end{array}\right]$$

$$= \left[\begin{array}{c|cccc|c} A & B_1 & B_2 & \cdots & B_m & B_0 \\ \hline C_1 & D_{11} & D_{12} & \cdots & D_{1m} & D_{10} \\ C_2 & D_{21} & D_{22} & \cdots & D_{2m} & D_{20} \\ \vdots & \vdots & \vdots & \ddots & \vdots & \vdots \\ C_p & D_{p1} & D_{p2} & \cdots & D_{pm} & D_{p0} \\ \hline C_0 & D_{01} & D_{02} & \cdots & D_{0m} & D_{00} \end{array}\right] \tag{15}$$

where the shorthand notation represents

$$P_{zw} = \left[\begin{array}{cccc} D_{11} & D_{12} & \cdots & D_{1m} \\ D_{21} & D_{22} & \cdots & D_{2m} \\ \vdots & \vdots & \ddots & \vdots \\ D_{p1} & D_{p2} & \cdots & D_{pm} \end{array}\right] + \left[\begin{array}{c} C_1 \\ C_2 \\ \vdots \\ C_p \end{array}\right]$$

$$\times (sI - A)^{-1}[B_1 \quad B_2 \quad \cdots \quad B_m]$$

$$P_{zu} = \left[\begin{array}{c} D_{10} \\ D_{20} \\ \vdots \\ D_{p0} \end{array}\right] + \left[\begin{array}{c} C_1 \\ C_2 \\ \vdots \\ C_p \end{array}\right](sI - A)^{-1}B_0 \tag{16}$$

$$P_{yw} = [D_{01} \quad D_{02} \cdots D_{0m}] + C_0(sI - A)^{-1}[B_1 \quad B_2 \cdots B_m]$$

$$P_{yu} = D_{00} + C_0(sI - A)^{-1}B_0$$

More explicitly, the augmented plant (15) represents the following system:

$$\dot{x} = Ax + B_0u + [B_1 \cdots B_m]w$$

$$y = C_0x + D_{00}u + [D_{01} \cdots D_{0m}]w \tag{17}$$

$$z = \left[\begin{array}{c} C_1 \\ \vdots \\ C_p \end{array}\right]x + \left[\begin{array}{c} D_{10} \\ \vdots \\ D_{p0} \end{array}\right]u + \left[\begin{array}{ccc} D_{11} & \cdots & D_{1m} \\ \vdots & & \vdots \\ D_{p1} & \cdots & D_{pm} \end{array}\right]w$$

Note that the subscript 0 is related to the plant and nonzero subscripts refer to different performance measures. To ensure the existence of stabilizing controllers, it is assumed that (A, B_0) is stabilizable and (C_0, A) is detectable. It is also assumed that all matrix partitionings are compatible. The augmented plant models (13) and (14) can be put into this form by realization of the transfer functions.

In recent years, many robust control design approaches have been proposed to account for uncertainties inherent in the system. The generalized Hamiltonian formulation[1,8] provides a unified framework for solving a class of robust controllers. One of the key results is the use of the generalized Hamiltonian to solve both H^2 and H^∞ problems. Although the analogy between H^2 and H^∞ has been exploited in Refs. 9–11, the generalized Hamiltonian formulation brings a new look to the structure and algorithms of these two control design methods. This approach aims to unify the performance of H^2 optimization, robustness due to H^∞ design, and the singularity property of singular control using one algorithm. Such a result is highly consistent with the overall system approach discussed in this section. In addition to the theoretical interest, the blending of various design methods greatly simplifies the implementation of computer aided design.

III. Robust Autopilot Design

Linearized missile dynamics models can be obtained by approximating the system dynamics around a given flight condition. The linear model of the HAVE DASH II missile has been derived in Ref. 1 and is denoted by

$$\dot{x} = Ax + Bu \tag{18}$$

where the state and control input are defined as

$$x = \left[\begin{array}{c} \alpha \\ q \\ \beta \\ r \\ p \\ \phi \end{array}\right], \qquad u = \left[\begin{array}{c} \delta_e \\ \delta_r \\ \delta_a \end{array}\right] \tag{19}$$

respectively. The state space matrices A and B are

$$A = \left[\begin{array}{cccccc} z_u & 1 & 0 & 0 & 0 & 0 \\ m_u & 0 & 0 & 0 & 0 & 0 \\ 0 & 0 & y_\beta & -\cos\alpha_0 & \sin\alpha_0 & g/V_m\cos\Theta_0 \\ 0 & 0 & n_\beta & 0 & 0 & 0 \\ 0 & 0 & l_\beta & 0 & 0 & 0 \\ 0 & 0 & 0 & 0 & 1 & 0 \end{array}\right]$$

$$B = \left[\begin{array}{ccc} z_{\delta_e} & z_{\delta_r} & z_{\delta_a} \\ m_{\delta_e} & m_{\delta_r} & m_{\delta_a} \\ 0 & y_{\delta_r} & y_{\delta_a} \\ 0 & n_{\delta_r} & n_{\delta_a} \\ 0 & l_{\delta_r} & l_{\delta_a} \\ 0 & 0 & 0 \end{array}\right] \tag{20}$$

respectively. Note that the autopilot delivers fin deflection commands based on the commands from the guidance law. The bank-to-turn logic transfers the linear acceleration commands from the

Table 1 Stability derivatives of HAVE DASH II missile

Stability derivatives	Flight conditions 1 $\alpha_0 = 2$ deg	2 $\alpha_0 = 5$ deg	3 $\alpha_0 = 10$ deg	4 $\alpha_0 = 15$ deg	5 $\alpha_0 = 20$ deg
z_α	−0.4083	−0.5673	−0.8196	−1.1372	−1.2342
z_{δ_e}	−0.1301	−0.1292	−0.1337	−0.1123	−0.1294
z_{δ_r}	−0.0028	−0.0066	−0.0066	−0.0092	−0.0068
z_{δ_a}	−0.0029	−0.0060	−0.0078	−0.0078	−0.0074
m_α	−24.1593	−38.7292	94.8788	−36.0662	−43.3763
m_{δ_e}	−149.9028	−149.4325	−155.6843	−139.6265	−157.6747
m_{δ_r}	−4.7630	−7.5668	−2.4725	−1.8821	−1.4831
m_{δ_a}	−4.1447	−6.8855	−3.2771	−2.1629	0.1519
y_β	−0.2298	−0.2518	−0.2980	−0.3286	−0.3086
y_{δ_r}	0.1133	0.1111	0.1021	0.0687	0.0741
y_{δ_a}	−0.0030	−0.0047	0.0025	0.0402	0.0447
n_β	−1.9531	2.5679	8.1743	−75.7856	−155.6500
n_{δ_r}	−132.6116	−129.7860	−117.2795	−78.7773	−87.6981
n_{δ_a}	4.8379	8.3528	4.2661	−39.1583	−46.3717
l_β	487.1155	−146.7585	−2075.6121	−1689.5171	−2583.0662
l_{δ_r}	−153.5108	−194.2953	−486.4590	−1221.5885	−1524.0958
l_{δ_a}	−2631.8740	−2671.2722	−2631.4756	−2243.1475	−2492.1411

guidance law to the angle-of-attack command α_c and the roll rate command Ω_c needed by the autopilot. Note that an α and β feedback has several advantages compared to the more conventional acceleration and angular velocity-loop closures, however, since angle-of-attack and sideslip angles are not readily measured with appropriate bandwidth by a typical missile system, effective α, β estimation needs to be designed.[12] The missile is assumed to fly at 40 k ft at 2.75 Mach. Five flight conditions are selected according to the angle of attack. Table 1 gives the stability derivatives at different angles of attack. It is observed that the linear model undergoes severe variations with respect to different flight conditions. Especially, notice the variations of m_α, which cause the pitch dynamics to become unstable at flight condition 3, and variations of the terms n_β, l_β, and l_{δ_r}, which are coupling terms in the roll-yaw dynamics.

The key requirement in missile autopilot design is to achieve robust performance and stability in the presence of uncertainties. These design concerns and requirements can be lumped into a canonical design formulation as discussed in Sec. II. In this section, robust autopilot design results are demonstrated. A class of robust designs are applied to the HAVE DASH II missile autopilot design. These include the H^2 design, GSLQ design, and H^∞ design.

A. H^2 Autopilot Design

Pitch Autopilot

The missile pitch dynamics are given by

$$\begin{bmatrix} \dot{\alpha} \\ \dot{q} \end{bmatrix} = \begin{bmatrix} z_\alpha & 1 \\ m_\alpha & 0 \end{bmatrix} \begin{bmatrix} \alpha \\ q \end{bmatrix} + \begin{bmatrix} z_{\delta_e} \\ m_{\delta_e} \end{bmatrix} \delta_e \tag{21}$$

To follow the commanded angle of attack α_c and achieve zero steady-state tracking error, the integral of the angle of attack is augmented as a state. The missile dynamics become

$$\begin{bmatrix} \dot{\alpha} \\ \dot{q} \\ \dot{\alpha}_i \end{bmatrix} = \underbrace{\begin{bmatrix} z_\alpha & 1 & 0 \\ m_\alpha & 0 & 0 \\ 1 & 0 & 0 \end{bmatrix}}_{A} \underbrace{\begin{bmatrix} \alpha \\ q \\ \alpha_i \end{bmatrix}}_{x} + \underbrace{\begin{bmatrix} z_{\delta_e} \\ m_{\delta_e} \\ 0 \end{bmatrix}}_{B_0} \underbrace{\delta_e}_{u} \tag{22}$$

The design objective is to minimize the following performance index:

$$J = \int_0^\infty z^T z + \rho \delta_e^2 \, dt \tag{23}$$

where ρ is the weighting on the control. To shape the angle-of-attack response, z is chosen to be of the form

$$z = [2\zeta\omega \quad 1 \quad \omega^2] \begin{bmatrix} \alpha \\ q \\ \alpha_i \end{bmatrix} \tag{24}$$

where ζ and ω are also design parameters. In this case

$$C_1 = \begin{bmatrix} 2\sqrt{\rho_1}\zeta\omega & \sqrt{\rho_1} & \omega^2 \\ 0 & 0 & 0 \end{bmatrix}$$
$$D_{10} = \begin{bmatrix} 0 \\ \sqrt{\rho_2} \end{bmatrix} \tag{25}$$

Strictly speaking, the robustness toward parameter variations is not guaranteed in this design. However, the results seem to be highly robust against parameter variations. The time responses of a H^2-controlled pitch system at five flight conditions is provided in Fig. 4a. The controller is designed at flight condition 3, the design parameters are selected as $\zeta = 0.7$, $\omega = 23.0$, and $\rho = 100$. In this evaluation, an actuator model $[180/(s + 180)]$ is included. The angle-of-attack command α_c enters the missile dynamics and autopilot through the angle-of-attack error integration $\int \alpha - \alpha_c$. That is, in a real implementation, the augmentation state becomes a filter used to nullify the steady-state tracking error. A nonlinear six-degree-of-freedom simulation has been conducted which simulates the autopilot under the missile full dynamics. The fixed gain controller does indeed achieve a robust angle-of-attack command following response, as shown in Fig. 4b. The angle-of-attack command is assumed to be 20 deg during the period from 1 s to 3 s, which is shown in the dashed line in the upper-left plot. The initial condition of the missile is assumed to be at 0-deg angle of attack, 40 k ft, and Mach 2.75. At the end of the maneuver, the Mach number has dropped to 2.31. Thus, although the variation of the Mach number is not addressed in the design, the controller appears to be insensitive toward Mach variation.

H^2 Roll-Yaw Autopilot

The roll-yaw dynamics are described by

$$\begin{bmatrix} \dot{\beta} \\ \dot{r} \\ \dot{p} \\ \dot{\phi} \end{bmatrix} = \underbrace{\begin{bmatrix} y_\beta & -\cos\alpha_0 & \sin\alpha_0 & g/V_m \cos\Theta_0 \\ n_\beta & 0 & 0 & 0 \\ l_\beta & 0 & 0 & 0 \\ 0 & 0 & 1 & 0 \end{bmatrix}}_{A} \underbrace{\begin{bmatrix} \beta \\ r \\ p \\ \phi \end{bmatrix}}_{x} + \underbrace{\begin{bmatrix} y_{\delta_r} & y_{\delta_a} \\ n_{\delta_r} & n_{\delta_a} \\ l_{\delta_r} & l_{\delta_a} \\ 0 & 0 \end{bmatrix}}_{B_0} \underbrace{\begin{bmatrix} \delta_r \\ \delta_a \end{bmatrix}}_{u} \tag{26}$$

The objective of the control is to have the roll rate p follow the

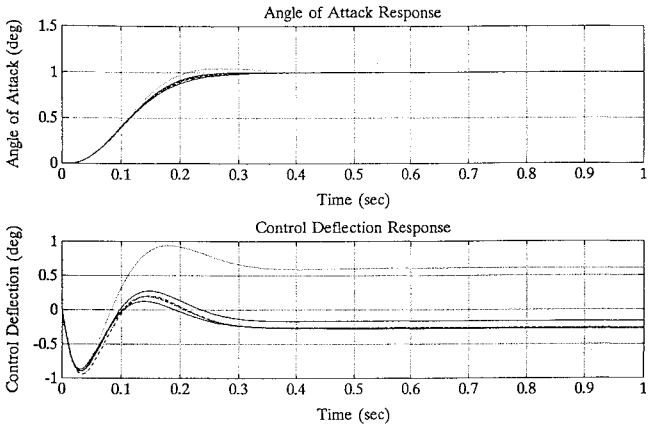

Fig. 4a H^2 pitch autopilot time response.

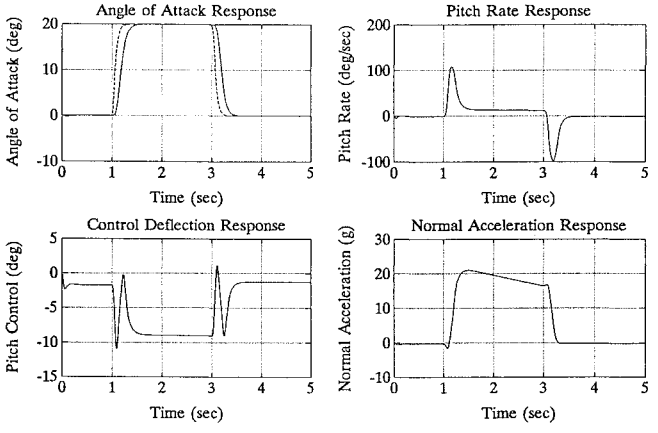

Fig. 4b H^2 pitch autopilot nonlinear simulation.

command roll rate Ω_c. The objective function of the roll-yaw H^2 design is selected as

$$J = \int_0^\infty z^T z + u^T R u \, dt,$$

$$z = \begin{bmatrix} \rho_1(\dot{\beta} + \lambda_\beta \beta) \\ \rho_2 r \\ \rho_3(p + \lambda_p \phi) \end{bmatrix} \qquad R = \begin{bmatrix} \rho_4 & 0 \\ 0 & \rho_5 \end{bmatrix} \tag{27}$$

The first term in z is to characterize the sideslip response. By placing a transmission zero at $-\lambda_\beta$, the closed-loop system, after the H^2 optimization, has a pole at $-\lambda_\beta$. The third term utilizes the transmission zero (or frequency-dependent weighting) concept to shape the roll response. The matrix R in the objective function is to adjust the control activity. The performance corresponds to

$$C_1 = \begin{bmatrix} \sqrt{\rho_1}(A_{11} + \lambda_\beta) & \sqrt{\rho_1}A_{12} & \sqrt{\rho_1}A_{13} & \sqrt{\rho_1}A_{14} \\ 0 & \sqrt{\rho_2} & 0 & 0 \\ 0 & 0 & \sqrt{\rho_3} & \sqrt{\rho_3}\lambda_p \\ 0 & 0 & 0 & 0 \\ 0 & 0 & 0 & 0 \end{bmatrix}$$

$$D_{10} = \begin{bmatrix} \sqrt{\rho_1}B_{11} & \sqrt{\rho_1}B_{12} \\ 0 & 0 \\ 0 & 0 \\ \sqrt{\rho_4} & 0 \\ 0 & \sqrt{\rho_5} \end{bmatrix} \tag{28}$$

where A_{ij} and B_{ij} are the (i, j)th entries of A and B, respectively. After some iterations, the following parameters are determined: $\lambda_\beta = 15.0$, $\lambda_p = 18.0$, $\rho_1 = 7.0$, $\rho_2 = 1.0$, $\rho_3 = 2.0$, $\rho_4 = 20$, and

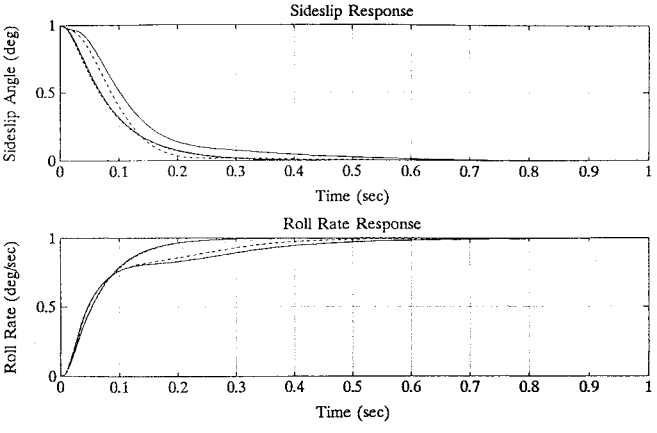

Fig. 4c H^2 roll-yaw autopilot time response.

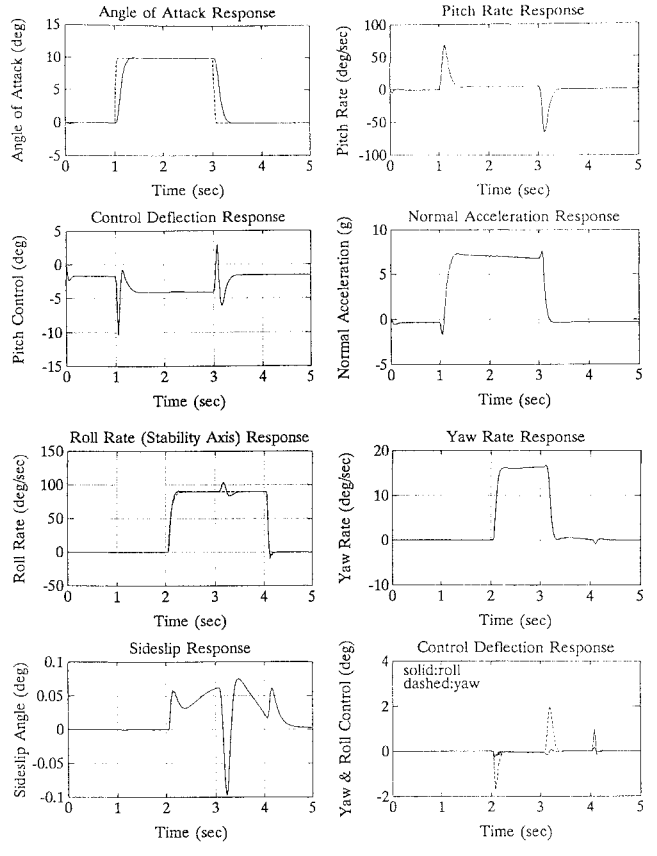

Fig. 4d H^2 autopilot six degree-of-freedom nonlinear simulation results.

$\rho_5 = 30$. The resulting controller is

$$\begin{bmatrix} \delta_r \\ \delta_a \end{bmatrix} = \begin{bmatrix} -5.0379 \\ 0.9181 \end{bmatrix} \beta + \begin{bmatrix} 0.4457 \\ -0.0560 \end{bmatrix} r + \left(\begin{bmatrix} -0.0008 \\ 0.0406 \end{bmatrix} + \frac{1}{s} \begin{bmatrix} 0.1859 \\ 0.5869 \end{bmatrix} \right) p \tag{29}$$

The resulting controller is evaluated to be robust against parameter variations. Two time responses are considered. One is the roll command response, another is the sideslip excursion response. With the fixed-gain linear quadratic controller, the responses at all five flight conditions are acceptable, as shown in Fig. 4c.

Finally, the nonlinear simulation results of the H^2 controller are provided in Fig. 4d. The commands in this nonlinear simulation include an angle-of-attack command, which has a value of 10 deg between 1.0 and 3.0 s, and a (stability axis) roll rate command of 90 deg/s between 2.0 and 4.0 s. The roll rate command and roll rate response are all in the stability axis. Again, the dashed line stands for

the command. The command following capability is achieved with a small amount of sideslip excursion. When the command levels are increased, the performance can still be achieved at a higher level of control deflections.

B. Generalized Singular Linear Quadratic Autopilot Design

In this section, the GSLQ approach is applied to the HAVE DASH II missile autopilot design. The design of the generalized singular linear quadratic control consists of selection of the steady-state manifold and control activity parameter. The criterion in selecting the steady-state manifold is that the system, when restricted in this manifold, is stable and has a satisfactory response. The control is effected by

$$u = (s + R_c)u^0 \tag{30}$$

where u^0 is the control determined by the steady-state manifold, and R_c is a design parameter. In the design, the following performance measure, which corresponds to the integrand in the objective function, is selected as

$$z = [2\zeta\omega \quad 1 \quad \omega^2]\begin{bmatrix}\alpha\\ q\\ \alpha_i\end{bmatrix} = \underbrace{[2\zeta\omega \quad 1 \quad \omega^2]}_{C_1}x \tag{31}$$

This ensures that the angle-of-attack response is approximated by a second-order system with damping ratio ζ and frequency ω. Naturally, the parameters ζ and ω are design parameters to be selected during the design. The problem of minimizing the H^2 norm of z is singular since there is no penalty on the control δ_e in the z term. Applying a structure algorithm, the transformed system matrices are

$$\begin{aligned} A^{(1)} &= A, & B_0^{(1)} &= AB_0 + R_cB_0,\\ C_1^{(1)} &= C_1, & D_{10}^{(1)} &= C_1B_0 \end{aligned} \tag{32}$$

where R_c is an adjustable parameter. Since $D_{10}^{(1)}$ is of full rank, by solving a regular H^2 problem, we can obtain a control gain $F^{(1)}$. Then the total gain is calculated from

$$F = R_cF^{(1)} + F^{(1)}A \tag{33}$$

It is noticed that by using this approach, a singular problem is transformed into a nonsingular one, in a very easy manner, and no decompositions are required. Some manipulations further reveal that the control δ_e is equal to

$$\begin{aligned}\delta_e &= \left(R_cF^{(1)} + F^{(1)}A\right)x\\ &= \frac{-1}{2\zeta\omega z_{\delta e} + m_{\delta e}}\left[\left(2\zeta\omega z_\alpha + m_\alpha + \omega^2 + 2\zeta\omega R_c\right)\alpha\right.\\ &\quad \left. + (2\zeta\omega + R_c)q + R_c\omega^2\alpha_i\right]\end{aligned} \tag{34}$$

which can be simplified as

$$\delta_e \approx (-1/m_{\delta e})\left[(\omega^2 + 2\zeta\omega R_c)\alpha + (2\zeta\omega + R_c)q + R_c\omega^2\alpha_i\right] \tag{35}$$

This approximation is valid as long as the parameters ω and R_c are selected such that $\omega^2 + 2\zeta\omega R_c$ dominates m_α. This domination also implies that the effect of m_α on the resulting system response is reduced. That is, the system is robust against variations of m_α. Another advantage of the control law is that the resultant control gain depends only on the control effectiveness and design parameters. With a simple scheduling device or control effectiveness estimator, the GSLQ pitch control can be readily implemented. A similar approach can be used to design the roll-yaw autopilot.

In the pitch design of the HAVE DASH II autopilot, the parameters $\zeta = 0.7$, $\omega = 23.0$, and $R_c = 18.0$ are chosen. The flight condition 3 ($\alpha_0 = 10$ deg) is selected as the nominal. Note that the parameters ω and R_c are selected such that $\omega^2 + 2\zeta\omega R_c$ is (much) larger than 150, the extent of the variations due to m_α. This design leads to the feedback

$$\delta_e = \left(7.1208 + \frac{61.1622}{s}\right)\alpha + 0.3224q \tag{36}$$

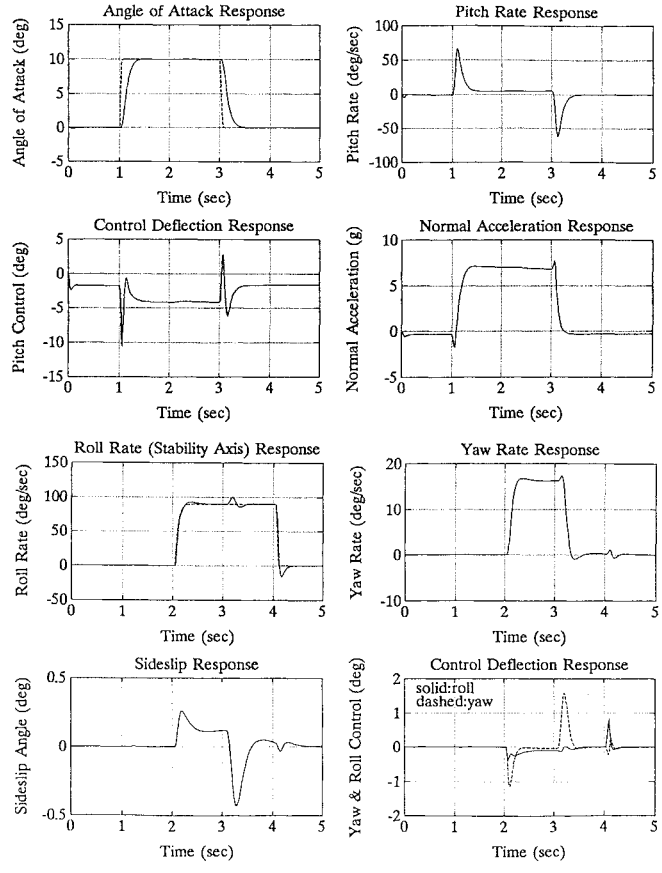

Fig. 5 GSLQ autopilot six-degree-of-freedom nonlinear simulation results.

The time responses of the GSLQ controller with respect to the missile dynamics are comparable with that of the H^2 design.

In the roll-yaw autopilot design, the singular performance index is chosen as

$$J = \int z^T z\,dt$$

with

$$z = C_1x = \begin{bmatrix}\lambda_\beta & 1 & 0 & 0\\ 0 & 0 & 1 & \lambda_p\end{bmatrix}x \tag{37}$$

The control activity parameter R_c is chosen to be of the diagonal form

$$R_c = \begin{bmatrix}k_1 & 0\\ 0 & k_2\end{bmatrix} \tag{38}$$

With the flight condition at 5 deg of the angle of attack selected as the nominal one, the GSLQ control leads to the roll-yaw autopilot with $\lambda_\beta = -15$, $\lambda_p = 25$, $k_1 = 12$, and $k_2 = 20$.

The nonlinear simulation results of the combined pitch-roll-yaw autopilot are shown in Fig. 5. Satisfactory roll rate following response is achieved. The induced sideslip is small since the roll is performed along the stability axis. The body yaw rate for coordination is

$$R = \Omega_c \sin\alpha_c = 90 \times \sin(10\text{ deg}) = 15.62\text{ deg/s}$$

The control deflections of the yaw and roll devices are shown in the lower right-part of Fig. 5. More activity is involved in the yaw control device than in the roll since the fins are far more effective at producing roll than yaw (see Table 1).

C. H^∞ Autopilot Design Example

Pitch System Design

In the design, control activity, performance, and uncertainties are considered in selecting the performance index. The objective

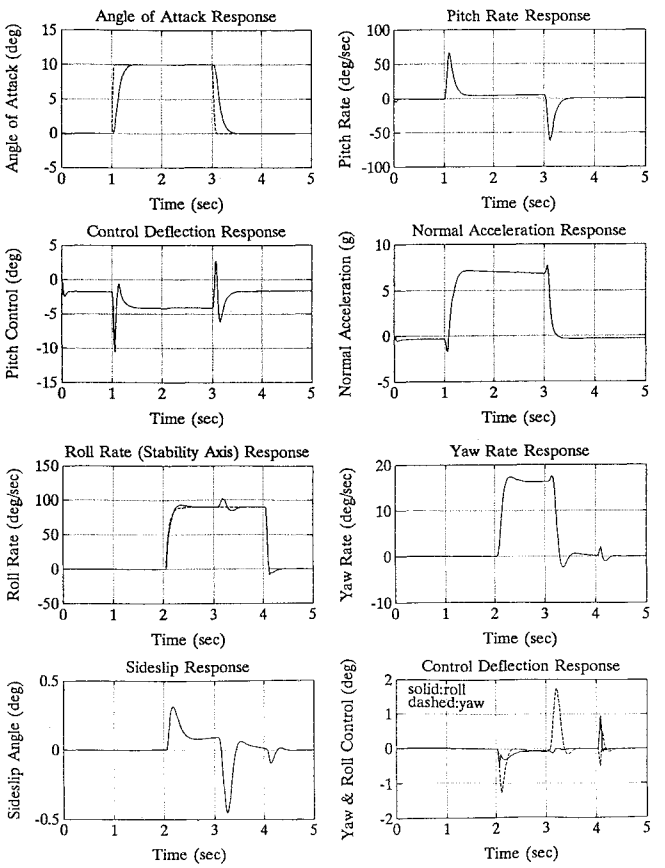

Fig. 6 H^∞ autopilot six-degree-of-freedom nonlinear simulation results.

measure to be minimized is selected to be

$$z = \underbrace{\begin{bmatrix} \bar{\rho}_1 & 0 & 0 \\ 0 & 0 & 0 \\ \kappa \times 2\zeta\omega & \kappa & \kappa\omega^2 \end{bmatrix}}_{C_1} x + \underbrace{\begin{bmatrix} 0 \\ \rho \\ 0 \end{bmatrix}}_{D_{10}} \delta_e \tag{39}$$

The first row of C_1 and the matrix

$$B_1 = \begin{bmatrix} 0 \\ 1 \\ 0 \end{bmatrix} \tag{40}$$

model the structure of the disturbance causing by the variations of m_α. In the design, $\bar{\rho}_1$ is chosen to be 150 to represent the extend of the parameter variation. The third element of z represents a measure, $q + 2\zeta\omega\alpha + \omega^2\alpha_i$, which is used to monitor the performance. Other parameters selected are $\zeta = 0.7$, $\omega = 23.0$, $\rho = 50.0$, and $\kappa = 7.0$. This gives the control law

$$\delta_e = \left(8.7780 + \frac{77.9565}{s}\right)\alpha + 0.3791q \tag{41}$$

Robust stability is achieved as supported by the nonlinear simulation results.

Roll-Yaw System Design

With $x = [\beta, r, p, \phi]^T$ as the state, the H^∞ design is to minimize the transfer function from the external disturbance to the performance measure. The performance measure is assumed to be

$$z = \underbrace{\begin{bmatrix} \bar{\rho}_2 & 0 & 0 & 0 \\ k_1\lambda_\beta & k_1 & 0 & 0 \\ 0 & 0 & k_2 & k_2\lambda_p \\ 0 & 0 & 0 & 0 \end{bmatrix}}_{C_1} x + \underbrace{\begin{bmatrix} 0 & 0 \\ 0 & 0 \\ 0 & 0 \\ \ell_{11} & \ell_{12} \\ \ell_{21} & \ell_{22} \end{bmatrix}}_{D_{10}} u \tag{42}$$

Similar to the pitch autopilot, the external disturbance is assumed to have the structure $B_1 = [0\ 1\ 0\ 0]^T$. Parameter $\bar{\rho}_2$ is chosen to be 250 to represent the extend of variation in l_β. Other parameters used in the design are $\lambda_\beta = -18.0$, $\lambda_p = 15.0$, $k_1 = 1$, $k_2 = 3.5$, $\ell_{11} = 50.0$, $\ell_{12} = -60.0$, $\ell_{21} = 120.0$, and $\ell_{22} = 160.0$. The controller is derived as

$$\begin{bmatrix} \delta_r \\ \delta_a \end{bmatrix} = \begin{bmatrix} -3.0726 \\ 1.0093 \end{bmatrix}\beta + \begin{bmatrix} 0.2395 \\ -0.0846 \end{bmatrix} r + \left(\begin{bmatrix} -0.0203 \\ 0.0325 \end{bmatrix} + \frac{1}{s}\begin{bmatrix} 0.0210 \\ 0.2954 \end{bmatrix} \right) p \tag{43}$$

The controller is solved using a generalized Hamiltonian formulation. No scalings are required in this approach. The nonlinear simulation result is provided in Fig. 6.

IV. Concluding Remarks

In this paper, the issue of the robust autopilot design has been discussed. The canonical design formulations for an autopilot loop and an integrated autopilot demonstrated the technique of inserting the practical concerns. Through a systematic, one-loop-at-a-time augmentation, the complex process of developing a formulation that encompasses practical concerns in the autopilot design becomes transparent. Three autopilot designs have been applied to the HAVE DASH II missile system. The simulation shows that they achieve good response against aerodynamic variations and significant kinematic and inertia couplings. Through these selected examples, the process of implementing advanced robust control technology in the autopilot design is exhibited. It is also demonstrated that a unified formulation, data structure, and solution algorithm can be shared among a class of robust control methods. This greatly simplifies the implementation of computer aided design.

Acknowledgments

Research was supported by Wright Laboratories Armament Directorate under Contracts F08635-90-C-0362, F08630-91-C-0055, F08630-92-C-0060, and F08630-93-C-0023. We would like to acknowledge the valuable contributions of Steve Osder of McDonnell Douglas Helicopter Systems to practical concerns related to our autopilot design.

References

[1]American GNC Corp., "High Performance, Adaptive, Robust BTT Missile Autopilot Design: Nonlinear, Adaptive, Robust Autopilot Design," Rept. to Air Force Armament Lab., Eglin AFB, Contract F08630-91-C-0055, Chatsworth, CA, March 1992.

[2]American GNC Corp., "High Performance, Adaptive, Robust BTT Missile Autopilot Design: Autopilot Design Results of the HAVE DASH II System," Rept. to Air Force Armament Lab., Eglin AFB, Contract F08630-91-C-0055, Chatsworth, CA, Dec. 1991.

[3]Cloutier, J. R., Evers, J. H., and Feeley, J. J., "An Assessment of Air-to-Air Missile Guidance and Control Technology," *Proceedings of the American Control Conference*, June 1988, pp. 133–142.

[4]Lin, C. F., *Modern Navigation, Guidance, and Control Processing*, Prentice-Hall, Englewood Cliffs, NJ, 1991.

[5]Lin, C. F., and Lee, S. P., "Robust Missile Autopilot Design Using a Generalized Singular Optimal Control Technique," *Journal of Guidance, Control, and Dynamics*, Vol. 8, No. 4, 1985, pp. 498–507.

[6]Wise, K. A., "Missile Autopilot Robustness Using the Real Multiloop Stability Margin," *Proceedings of the AIAA Guidance, Navigation, and Control Conference*, Pt. 2, AIAA, Washington, DC, Aug. 1990, pp. 232–241.

[7]Wise, K. A., and Poolla, K., "Missile Autopilot Design Using H_∞ Optimal Control with μ-Synthesis," *Proceedings of the American Control Conference*, June 1990, pp. 2362–2367.

[8]Lin, C. F., ed., *Advanced Control System Design*, Prentice Hall, Englewood Cliffs, NJ, 1994.

[9]Jonckheere, E. A., Juang, J. C., and Silverman, L. M., "Spectral Theory of the Linear Quadratic and H^∞ Problem," *Linear Algebra and Its Applications*, Vol. 122, No. 3, 1989.

[10]Jonckheere, E. A., and Juang, J. C., "Fast Computation of Achievable Performance in Mixed Sensitivity H^∞ Design," *IEEE Transactions on Automatic Control*, Vol. AC-32, 1987, pp. 896–906.

[11]Doyle, J. C., Zhou, K., and Bodenheimer, B., "Optimal Control with Mixed H_2 and H_∞ Performance Objectives," *Proceedings of the 1989 American Control Conference*, Pittsburgh, PA, 1989.

[12]Osder, S., Private communication, July 1994.